Research paper

Acta Neurobiol Exp 2016, 76: 53–65

ACTA NEUROBIOLOGIÆ EXPERIMENTALIS

Cerebellar cortex development in the *weaver* condition presents regional and age-dependent abnormalities without differences in Purkinje cells neurogenesis

Joaquín Martí[1]*, María C. Santa-Cruz[1], José P. Hervás[1], Shirley A. Bayer[2], Sandra Villegas[3]*

*[1] Departament de Biologia Cel.lular, de Fisiologia i d'Immunologia, Unidad de Citologia i d'Histologia, Facultat de Biociències, Universitat Autònoma de Barcelona, Barcelona, Spain, [2] Laboratory of Developmental Neurobiology, Indianapolis, USA, [3] Departament de Bioquímica i Biologia Molecular, Facultat de Biociències, Universitat Autònoma de Barcelona, Barcelona, Spain, * Email: joaquim.Martí.clua@uab.es, sandra.villegas@uab.cat*

Ataxias are neurological disorders associated with the degeneration of Purkinje cells (PCs). Homozygous *weaver* mice (*wv/wv*) have been proposed as a model for hereditary cerebellar ataxia because they present motor abnormalities and PC loss. To ascertain the physiopathology of the *weaver* condition, the development of the cerebellar cortex lobes was examined at postnatal day (P): P8, P20 and P90. Three approaches were used:

1) quantitative determination of several cerebellar features;

2) qualitative evaluation of the developmental changes occurring in the cortical lobes; and

3) autoradiographic analyses of PC generation and placement.

Our results revealed a reduction in the size of the *wv/wv* cerebellum as a whole, confirming previous results. However, as distinguished from these reports, we observed that quantified parameters contribute differently to the abnormal growth of the *wv/wv* cerebellar lobes. Qualitative analysis showed anomalies in *wv/wv* cerebellar cytoarchitecture, depending on the age and lobe analyzed. Such abnormalities included the presence of the external granular layer after P20 and, at P90, ectopic cells located in the molecular layer following several placement patterns. Finally, we obtained autoradiographic evidence that wild-type and *wv/wv* PCs presented similar neurogenetic timetables, as reported. However, the innovative character of this current work lies in the fact that the neurogenetic gradients of *wv/wv* PCs were not modified from P8 to P90. A tendency for the accumulation of late-formed PCs in the anterior and posterior lobes was found, whereas early-generated PCs were concentrated in the central and inferior lobes. These data suggested that *wv/wv* PCs may migrate properly to their final destinations. The extrapolation of our results to patients affected with cerebellar ataxias suggests that all cerebellar cortex lobes are affected with several age-dependent alterations in cytoarchitectonics. We also propose that PC loss may be regionally variable and not related to their neurogenetic timetables.

Key words: cerebellar ataxias; homozygous *weaver* mice; development; cerebellar lobes; morphometry; [^{3}H]TdR autoradiography.

INTRODUCTION

The cerebellum is involved not only in motor coordination and motor learning, but it also plays an important role in the processing of the signal for perception, cognition and affective functions (Reeber et al. 2013). The cerebellum is composed by a limited number of cellular types that are characterized by distinctive morphology and molecular markers (Goldowitz and Hamre 1998, Schilling et al. 2008, Chetodal 2010). Many lines of evidence indicate that GABAergic neurons, such as Purkinje cells (PCs), inhibitory interneurons and deep cerebellar nuclei (DCN) neurons originate from the cerebellar neuroepithelium. By contrast, glutamatergic neurons, including unipolar brush cells, the projection neurons of the precerebellar nuclei, and also DCN neurons arise from progenitors located in the rhombic lip (Leto et al. 2012, Wullimann et al. 2011). Granule cells (GCs) precursors also emerge from the rhombic lip and they migrate tangentially over the piamater to form the external granule layer (EGL) (Altman and Bayer 1997).

Cerebellar disorders such as ataxias are severe neurological conditions that comprise a wide spectrum of diseases characterized by motor incoordination, imbalance and degeneration of PCs (Grüsser-Cornehls and Bäule 2001, Manto and Marmolino 2009, Cedelin 2014).

Received 21 June 2015, accepted 11 March 2016

Correspondence should be addressed to J. Martí and S. Villegas
Email: joaquim.Martí.clua@uab.es, sandra.villegas@uab.cat

Since these illnesses show both high morbidity and large socio-economic impact, it is imperative to use animal models to look at what environmental and/or genetic factors may be related to such conditions.

Weaver (*wv*) is a missense point mutation in the *Kcnj6* gene, which has been cloned and mapped to mouse chromosome 16 (Cheng et al. 1988, Reeves et al. 1989). The *Kcnj6* gene encodes the subunit of the homotetrameric potassium channel GIRK2 (Whorton and MacKinnon 2013). The difference between normal and *weaver* GIRK2 protein is one amino acid, a glycine to serine substitution in the middle of the pore-forming H5 region of the channel (Patil et al. 1995).

The homozygous *weaver* mice (*wv/wv*) present small size, instability of gait, weakness and hypotonia. Most of the males are sterile due to the loss of germinal and Sertoli cell (Harrison and Roffler-Tarlov 1988, Verina et al. 1995). In the central nervous system, the expression of the *weaver* gene has consequences for the olfactory bulb, where malpositioned and supernumerary cells are present in the external plexiform layer (Schein et al. 1998). At the hippocampus, the pyramidal cell layer of the *cornus ammonis* 3 region appears thicker than in normal mice, and presents ectopic clusters of pyramidal cells (Sekigucchi et al. 1995). The *weaver* homozygotes also present depletion of dopamine neurons in several midbrain areas including the substantia nigra pars compacta and the ventral tegmental area (Triarhou et al. 1988, Cavalcanti-Kwiatkoski et al. 2010).

The *weaver* homozygotes have been studied as an animal model of cerebellar disorders such as hereditary ataxias (Grüsser-Cornehls and Bäule 2001, Manto and Marmolino 2009, Cedelin 2014). GIRK2 is expressed, in the *weaver* cerebellum, from embryonic day 15 to postnatal day 20 (Wei et al. 1997). Mutant mice show degeneration of pontocerebellar mossy fibers and neuronal death in the pontine nuclei (Ozaki et al. 2002). In the cerebellum, *wv/wv* present severe depletion of GCs, PCs and DCN neurons (Rakic and Sidman 1973a, 1973b, Blatt and Eisenman 1985, Herrup and Trenkner 1987, Eisenman et al. 1998, Maricich et al. 1997, Martí et al. 2001, Lalonde and Strazielle 2007). The loss of PCs in the *weaver* homozygotes is observed as early as embryonic day 19 (Bayer et al. 1996). Interestingly, neuron demise is regionally variable, the vermis being the most impaired region, whereas cell depletion is spared at the hemispheres (Herrup and Trenkner 1987, Eisenman et al. 1998, Martí et al. 2001). Other alterations in the *weaver* cerebellum include: ectopic location of the surviving neurons, altered foliar patterns and aberrant cytoarchitecture of the cerebellar cortex (Rakic and Sidman 1973a, 1973b).

Therefore, GIRK2 is expressed from the prenatal life to the adulthood in multiple regions of the central nervous system and its expression is not limited to the neuronal populations that are susceptible to degeneration (Wei et al. 1997). Two models have been proposed to explain how the *wv* mutation produces the depletion of neurons (Harkins and Fox 2002). The first of them proposes that the *weaver* condition leads to a constitutively active GIRK2 channel, which results in the loss of selectivity for K^+ allowing Na^+ and Ca^{2+} to penetrate cells. Neuronal death is related to the elevated intracellular Ca^{2+} levels caused by continuous depolarization. The second model suggests the loss of the GIRK2*wv* channel function, which reduces a major inhibitory pathway in developing neurons, producing hyperexcitability and cell death.

In light of the above, we began a set of experiments. The objective of this article is therefore to study the postnatal development of the cerebellar cortex lobes in the *weaver* condition as a means of shedding new light on how the expression of the *weaver* gene affects the development of the cerebellum. Moreover, using the *weaver* animal model, we extrapolate the results of our experiments to patients affected with cerebellar disorders such as hereditary ataxias. Three aspects were addressed.

1) We quantitatively determined several cerebellar parameters in the *weaver* homozygotes at postnatal day (P) P8, P20 and P90. The features determined were the length of the cerebellar cortex; the area of the EGL; the area of the molecular layer (ML); and the number of PCs.

2) We qualitatively studied the developmental changes occurring in the cerebellum of the *weaver* homozygotes at the above-mentioned survival times.

3) Through a progressively delayed cumulative labeling method, we studied the production and final location of PCs in *wv/wv* exposed to [^{3}H]TdR as embryos, to determine possible differences among animals collected at P8, P20 and P90.

These ages were not selected at random but, instead, selected because in wild-type mice it is at about P8 when the EGL reaches its greatest thickness, PCs are dispersed into a monolayer, and a clearly delineated granule layer is seen. At P20, the EGL has virtually disappeared and PCs have established a complex interaction network with the microneurons that results in the proper wiring of the fine circuitry in the cerebellar cortex (Altman and Bayer 1997). We arbitrarily establish adulthood at P90. Finally, the *quadrupartite* anteroposterior parcellation of the cerebellar cortex was chosen because the anterior lobe is a nonhemipheric component of the cerebellar cortex. In contrast, the central lobe is the most progressive component in the sense that it is related to the expanding cerebellar hemispheres. The posterior lobe is linked to the paraflocculus and the inferior lobe and the lateral flocculus constitute the vestibulocerebellum (Altman and Bayer 1997).

METHODS

Animals and experimental design

All mice were obtained from the colony of control (+/+) and *weaver* (*wv/wv*) mice at Indiana University School of Medicine maintained on the B6CBA-A^{w-j}/A hybrid stock. The parents of the +/+ and *wv/wv* offspring used in current study were either carried females (*wv*/+) or *wv/wv* females mated to *wv*/+ males. Each pregnant dam was subcutaneously injected between 8 and 9 AM on two successive days in an overlapping series with [^{3}H] TdR (5 μCi/g of body weight, New England Nuclear #NET-027) on consecutive days during the time when PCs were being generated, according to the following time-window: embryonic day (E)11–12, E12–13, E13–14 and E14–15. No *wv*/+ were included in the study. Seven offspring from different dams were used for each experimental group (+/+ and *wv/wv*) and time-window (from E11–12 to E14–15). Standard laboratory conditions (food and water *ad lib*, 22±2ºC, 12 h light: dark cycle starting at 8:00 AM) were used. Animal cure and experimentation were conducted in accordance with the Ethical Committee of the Indiana-Purdue University.

Wv mutation was ascertained by means of single-strand conformational polymorphism (Wei et al. 1996). Phenotypes were identified taking their motor abnormalities into account (Lalonde and Strazielle 2007) as well as by microscopic examination of the cerebellum, which showed disorganized cytoarchitecture as a consequence of the depletion of several neuron populations (Rakic and Sidman 1973a, 1973b).

Tissue processing

At P8, P20 and P90, pups were anesthetized with sodium pentobarbital (50 mg/kg of body weight) and perfused through the heart with 10% neutral buffered formalin. Tissue processing was developed as regular procedures from our laboratory. The blocks containing the cerebellum were sectioned at 10 μm in the sagittal plane and one out of every six sections was collected to preclude the overcounting of neurons. Only those sections representative of the medial point of the vermis were used in the study. This region is characterized by the limited presence of fastigial nucleus. No sections containing cerebellar hemispheres were studied.

Morphometry of the cerebellum

The following features of the cerebellar morphology were separately quantified in every lobe of the cerebellar cortex (anterior, central, posterior and inferior): the length of the cerebellar cortex, the area of the EGL, the area of the ML and the number of PCs. Each parameter was determined in three sections of every experimental animal and data were added to obtain a mean per mouse. With this information, means were calculated for each experimental group.

Measurements were done as previously reported (Martí et al. 2013). Under identical lighting conditions, images were captured by a CCD-IRIS color video camera (Sony, Japan) coupled to a Zeiss Axiosphot microscope and digitalized. Morphometric analysis was performed with the Visilog 5 software (Noesis, France). Analysis was done as follows: the first step was calibration to convert pixel units to metric units. Subsequently, the length of the cerebellar cortex and the contour of the EGL and the ML were manually delimited to obtain initial binary images. These images were submitted to the mentioned software to accurately measure the length of the cerebellar cortex and the area of the EGL and ML in every analyzed region.

Qualitative analyzes of the cerebellar cortex

Light microscopic analyses were made with a Zeiss Axiosphot microscope using a wide set of objectives ranging from 2.5 to 63X. Observations were focused at the foliar crowns from the anterior lobe (lobules I, III and V), the central lobe (VII and VIII), the posterior lobe (IX) and the inferior lobe (X). The depth of the prima, secunda and posterolateralis fissures was also measured.

The limits between foliar crowns and fissures were set as previously reported (Wahlsten and Andison 1991, Martí et al. 2007). This consisted of digitally capturing images from wild-type and homozygous *weaver* mice cerebella with a CCD-IRIS color video camera (Sony, Japan) coupled to a Zeiss Axiosphot microscope equipped with a 40X objective. By means of software (Visilog 5, Noesis, France) two outlines were drawn. The first of these delimited the cerebellar cortex surface, while the second was done by tracing the angle bisector in a given fissure corner. The points of intersection on both sides represented the two outer limits of the fissure. The space included between two successive fissures was considered as a foliar crown.

Observations were carried out in 14 *wv/wv* mice from different dams (7 from the E14–15 and 7 from the E15–16 [^{3}H]TdR time-windows). Three sections per mouse were studied. These injection series were chosen because they presented very low [^{3}H]TdR labeling and cerebella stand out very clearly in the sections. The names of the lobes and lobules used are those previously assigned (Larsell 1952, Altman and Bayer 1997).

[^{3}H]TdR autoradiography

Isotope incorporation was assessed with a previously described method (Martí et al. 2002, 2009). This consisted of coating the slides with a liquid photographic emulsion (undiluted Kodak NTB3) in a darkroom illustrated by Kodak Series 2 dark-red safelights, drying them in a humidified atmosphere, and storing them in light-tight boxes in the refrigerator for an exposure period of 12 weeks. The slides were developed in a Kodak D-19, and were then post-stained with haematoxylin, dehydrated, and cover-slipped with Permount. Labeled PCs could be identified by the cluster of reduced silver grains (black granules) over their nuclei. Neurons with seven grains or more per nucleus were considered labeled (Fig. 1).

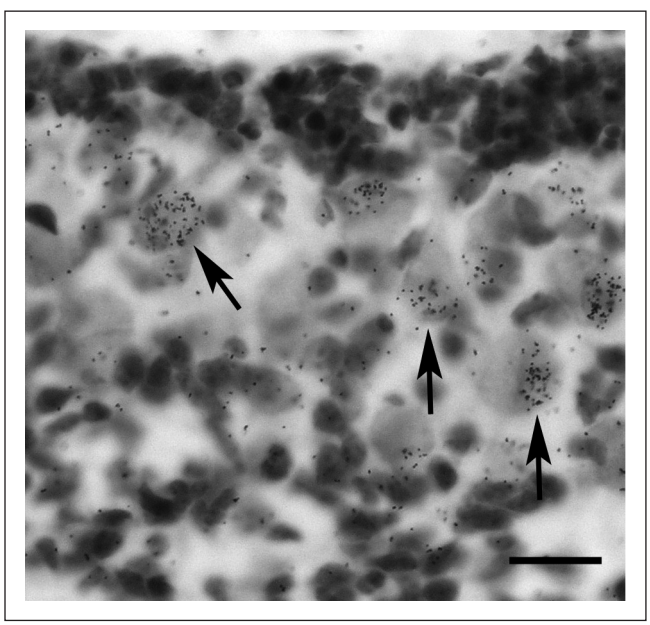

Fig 1. High-magnification autoradiogram from a homozygous *weaver* mouse exposed to [^{3}H]TdR on E12–13 and killed at postnatal day 8. Labeled Purkinje cells can be identified by the presence of nuclear black dots (arrows). Note the external germinal layer at the top of the photograph. Scale bar – 30 mm.

Cell counts

Counts of PCs were carried out by visual scanning of the cerebellar cortex throughout the entire anteroposterior profile of any given folium. Criteria for scoring PCs included the presence of a large and clear nucleus, pear-shaped cell body and distinctive stain properties. Since *wv*/*wv* PCs somata are ectopically settled due to the disruption of the normal cerebellar cortex cytoarchitecture, it becomes difficult to distinguish between PCs and any other large neurons. Total PC counts in the mutant animals were therefore multiplied by a Golgi-cell correction factor (85.7%). This correction factor was derived from PCs/Golgi cell ratio in lower mammals (Lange 1982) and it has been used in previous quantitative analyses of *weaver* PCs (Blatt and Eisenmann 1985, Martí et al. 2007, 2013).

Labeled and unlabeled PCs were separately counted. The frequency of [^{3}H]TdR-labeled neurons was calculated as the percentage of the total number of scored PCs. To infer PCs neurogenetic timetables, a modification of the progressively delayed comprehensive labeling procedure was used (Bayer and Altman 1987).

Statistical Treatment

Data analyzes were carried out using SPSS (version 18) statistical software. Two-way ANOVAs with "genotype" (+/+ and *wv*/*wv*) and "age" (P8, P20 and P90) as the main factors were used for analyzing the quantified features of the cerebellum as well as the autoradiographic results. Further statistical significance of inter-genotypes or inter-ages differences were determined with the one-way ANOVA followed by individual comparison of means with the Student-Newman-Keuls (SNK) test. If only two means were compared the Student's *t*-test (*t*-test) or the Mann-Whitney U-test (*U*-test) were used. A '*P*' value less than 0.05 was considered statistically significant.

RESULTS

Quantifications in the cerebellar cortex

Data concerning to the length of the cerebellar cortex, the area of the EGL, the area of the ML and the number of PCs per section in the anterior, central, posterior and inferior lobes of the cerebellar cortex are presented in Table I. Results of the two-way ANOVA of the former parameters are depicted in Table II.

Significant effects of the genotype were found in all of the features analyzed in the cerebellar cortex. The effects of age reached statistical significance in the case of the length of the cerebellar cortex and the area of the ML. No effect of this main factor on the number of PCs was observed, indicating that the depletion of these macroneurons in the *weaver* homozygotes is not progressive with age at least in the survival times analyzed in the present study. The interaction genotype X age was statistically significant depending on the quantified parameter. Thus, it was significant for the length of the cerebellar cortex in the anterior and inferior lobes, whereas significance for the area of the ML was found in all of the analyzed lobes except for the anterior one.

Table I. Mean values for several features in the anterior, central, posterior and inferior lobes of the cerebellar cortex

ANTERIOR LOBE								
	Length (mm)		EGL area (μm²)		ML area (μm²)		PCs number	
age	+/+	*wv/wv*	+/+	*wv/wv*	+/+	*wv/wv*	+/+	*wv/wv*
P8(14)	14.0±0.5[a]	4.4±0.3[a,*]	184.5±6.2	44.7±3.7[a,*]	280.6±9.2[a]	38.1±4.3[a,*]	313.2±3.1[a]	97.5±1.8[a,*]
P20(14)	19.5±0.4[b]	7.1±0.3[b,*]	0±0	32.5±1.4[b,*]	408.6±17.5[b]	182.9±10.6[b,*]	320.2±3.4[a]	94.4±2.3[a,*]
P90(14)	23.6±0.8[c]	8.5±0.6[b,*]	0±0	0±0	465.3±13.2[c]	233.6±12.8[c,*]	317.9±5.7[a]	97.4±1.8[a,*]
CENTRAL LOBE								
age	+/+	*wv/wv*	+/+	*wv/wv*	+/+	*wv/wv*	+/+	*wv/wv*
P8(14)	9.1±0.3[a]	1.9±0.2[a,*]	163.2±5.4	48.3±3.9[a,*]	269.3±8.8[a]	23.0±1.9[a,*]	213.2±5.5[a]	41.8±2.1[a,*]
P20(14)	12.3±0.3[b]	3.1±0.2[b,*]	0±0	32.5±1.4[b,*]	392.3±16.8[b]	116.1±6.8[b,*]	218.0±6.1[a]	40.5±2.5[a,*]
P90(14)	15.4±0.2[c]	3.6±0.3[b,*]	0±0	0±0	446.7±12.7[c]	152.3±8.3[c,*]	216.4±10.4[a]	41.7±2.0[a,*]
POSTERIOR LOBE								
age	+/+	*wv/wv*	+/+	*wv/wv*	+/+	*wv/wv*	+/+	*wv/wv*
P8(14)	4.7±0.2[a]	0.7±0.03[a,*]	184.5±6.2	41.1±3.4[a,*]	274.9±8.9[a]	14.7±0.8[a,*]	99.9±2.6[a]	15.7±0.8[a,*]
P2(14)	6.7±0.1[b]	1.1±0.1[b,*]	0±0	26.0±1.1[b,*]	400.5±17.1[b]	62.5±3.6[b,*]	102.2±2.8[a]	15.2±0.9[a,*]
P90(14)	8.6±0.3[c]	1.3±0.1[b,*]	0±0	0±0	455.9±12.9[c]	77.8±4.3[b,*]	101.5±4.9[a]	15.7±0.9[a,*]
INFERIOR LOBE								
age	+/+	*wv/wv*	+/+	*wv/wv*	+/+	*wv/wv*	+/+	*wv/wv*
P8(14)	1.4±0.3[a]	0.9±0.2[a,*]	177.4±5.9	44.7±3.7[a,*]	297.3±9.7[a]	16.2±1.8[a,*]	39.7±1.1[a]	19.1±0.9[a,*]
P20(14)	1.8±0.3[b]	1.4±0.3[b,*]	0±0	35.1±1.5[b,*]	433.2±8.5[b]	84.8±4.9[b,*]	40.8±1.2[a]	18.5±1.2[a,*]
P90(14)	2.7±0.1[c]	1.7±0.2[c,*]	0±0	0±0	493.2±5.9[c]	113.1±6.2[b,*]	40.5±1.9[a]	19.1±0.9[a,*]

Mean ±SEM are indicated. P – postnatal day, EGL – external granular layer, ML – molecular layer, PCs – Purkinje cells. Groups tagged with different letters indicate statistically significant differences among postnatal day 8, 20 and 90 in the +/+ or *weaver* condition (one-way ANOVA followed by Student-Newman-Keuls), while those labeled with symbols denote significant differences with regard to wild-type (*t*-test or *U*-test). In parenthesis is the number of mice from different dams (7 of them were +/+ and 7 were *wv/wv*). The EGL, a temporary structure, already disappeared at postnatal day 20 for the +/+, whereas it did so at postnatal day 90 for the *vw/vw*.

Further comparisons (+/+ versus *wv/wv*) showed that the length of the cerebellar cortex, the area of the ML as well as the number of PCs were greater in the +/+ than in the *wv/wv* mice. This was found in all of the analyzed lobes at P8, P20 and P90. At P8, the area of the EGL was greater in the +/+ than in the *wv/wv* mice (*t*-test or the *U*-test, $P< 0.05$, tables I and II). In the case of PCs, data analysis revealed that the depletion of these macroneurons was regionally variable. The most important deficit was observed in the central and posterior lobes; whereas depletion was less observable in the anterior lobe and least observable in the inferior lobe.

Comparisons with the one-way ANOVA followed by the SNK-test revealed significant effects of the age on the cerebellar cortex length and ML area. The differences between P8 and P20 were statistically significant in the +/+ (*t*-test, $P<0.001$) and *wv/wv* (*t*-test, $P<0.01$) mice in all of the analyzed lobes. The same was seen between P20 and P90 when both parameters were taken into account in the +/+ mice (*t*-test, $P<0.001$). In the *weaver* homozygotes, on the other hand, differences were only observed in the ML area of the anterior, central and inferior lobes (*t*-test, $P<0.05$, see Tables I and II).

Post hoc comparisons revealed that, at P8, the EGL area was smaller in the *weaver* homozygotes than in the wild-type for all of the analyzed lobes (*t*-test or the *U*-test, $P<0.001$). In concordance with the temporal nature of this structure, it was already depleted of cells at P20 in the wild type, whereas in the *wv/wv* this feature was still observed.

Qualitative observations in the cerebellar cortex

Sagittal sections from +/+ and *wv/wv* cerebella illustrating the lobular organization of the cortex in each studied age are shown in Fig. 2. The +/+ cerebellum showed the characteristic pattern of fissures and foliar crowns in all of the analyzed ages. In the *weaver* homozygotes, the cerebellum was smaller than in their +/+ counterparts. Cardinal fissures determining the limits among the four lobes of the +/+ and *wv/wv* cerebellar cortex (prima, secunda and posterolateralis)

Table II. Results of the two-way ANOVA of the parameters studied in each lobe of the cerebellar cortex

ANTERIOR LOBE			
factor	cerebellar cortex length	molecular layer area	Purkinje cells number
genotype (G)	[$F_{1,36}$=931.6, P<0.001]	[$F_{1,36}$=571.4, P<0.001]	[$F_{1,36}$=991.6, P<0.001]
age (A)	[$F_{2,36}$=104.3, P<0.001]	[$F_{2,36}$=134.5, P<0.001]	NS
G×A	[$F_{2,36}$=3.52, P<0.04]	NS	NS
CENTRAL LOBE			
factor	cerebellar cortex length	molecular layer area	Purkinje cells number
genotype (G)	[$F_{1,36}$=1747, P<0.001]	[$F_{1,36}$=1381, P<0.001]	[$F_{1,36}$=785.7, P<0.001]
age (A)	[$F_{2,36}$=100.9, P<0.001]	[$F_{2,36}$=291.5, P<0.001]	NS
G×A	NS	[$F_{2,36}$=98.8, P<0.001]	NS
POSTERIOR LOBE			
factor	cerebellar cortex length	molecular layer area	Purkinje cells number
genotype (G)	[$F_{1,36}$=2480, P<0.001]	[$F_{1,36}$=1838, P<0.001]	[$F_{1,36}$=2723, P<0.001]
age (A)	[$F_{2,36}$=108.1, P<0.001]	[$F_{2,36}$=146.5, P<0.001]	NS
G×A	NS	[$F_{2,36}$=35.9, P<0.001]	NS
INFERIOR LOBE			
factor	cerebellar cortex length	molecular layer area	Purkinje cells number
genotype (G)	[$F_{1,36}$=161.1, P<0.001]	[$F_{1,36}$=1442, P<0.001]	[$F_{1,36}$=2156, P<0.001]
age (A)	[$F_{2,36}$=129.1, P<0.001]	[$F_{2,36}$=93.8, P<0.001]	NS
G×A	[$F_{2,36}$=13.8, P<0.001]	[$F_{2,36}$=12.1, P<0.001]	NS

NS – not significant.

were present, and easily distinguishable. A closer analysis revealed that, at P8, the +/+ cerebellar cortex exhibited its typical cytoarchitecture. However, when the observations were focused on the *wv/wv*, this structure did not exhibit the typical layering, which confirms early data (Herrup and Trenkner 1987, Eisenman et al. 1998, Armstrong and Hawkes 2001). In accordance with previous observations from our laboratory, it was found that the *wv/wv* EGL was present at P8 (Martí et al. 2013), although impaired in all of the areas. At P20, the cerebellar cortex of the *weaver* homozygotes continued being an aberrant structure in which the EGL was still present.

In those mutant mice collected at P90, the cytoarchitecture of the cerebellar cortex was similar to that observed at P20. In spite of that, there were important differences such as the disappearance of the EGL and the presence of GCs in the ML. The later followed, at least, the three patterns (Fig. 3, Table III):

1) superficial, in subpial position as well as in the middle-to-lower part of the ML,

2) middle-to-lower part of the ML, and

3) randomly placed throughout the ML. No ectopic GCs were observed in the +/+ mice. Patterns of ectopic GCs were similar in all of the *wv/wv* studied sections.

Developmental timetables and neurogenetic gradients of Purkinje cells

Sets of autoradiograms, from E11 to E15 ^{3}[H]TdR injections series, were used to address the possibility that there may be regional differences in PC production between +/+ and *wv/wv* mice. In this way, comparative evaluations concerning genotype (+/+ or *wv/wv*) and age (P8, P20 and P90) were separately done in each lobe of the cerebellar cortex. Statistical analysis of the data revealed effect neither of age nor genotype on the percentage of labeled PCs; similarly, no differences among lobes were found when a given time-window was considered. Fig. 4 graphically displays the proportion of labeled PCs obtained for each vermal lobe. From these set of histograms, it can be deduced:

1) the greatest incidence of *wv/wv* labeled neurons occurred when their generation periods were just beginning, i.e., on the E11–E12 time-window,

2) the percentage of tagged *wv/wv* PCs dropped quickly from injections on E11–12 to E14–15, and

3) when ^{3}[H]TdR injections were supplied on E14–15, the percentages of labeled *wv/wv* PCs were very low, indicating that the actual period of generation for these macroneurons was over.

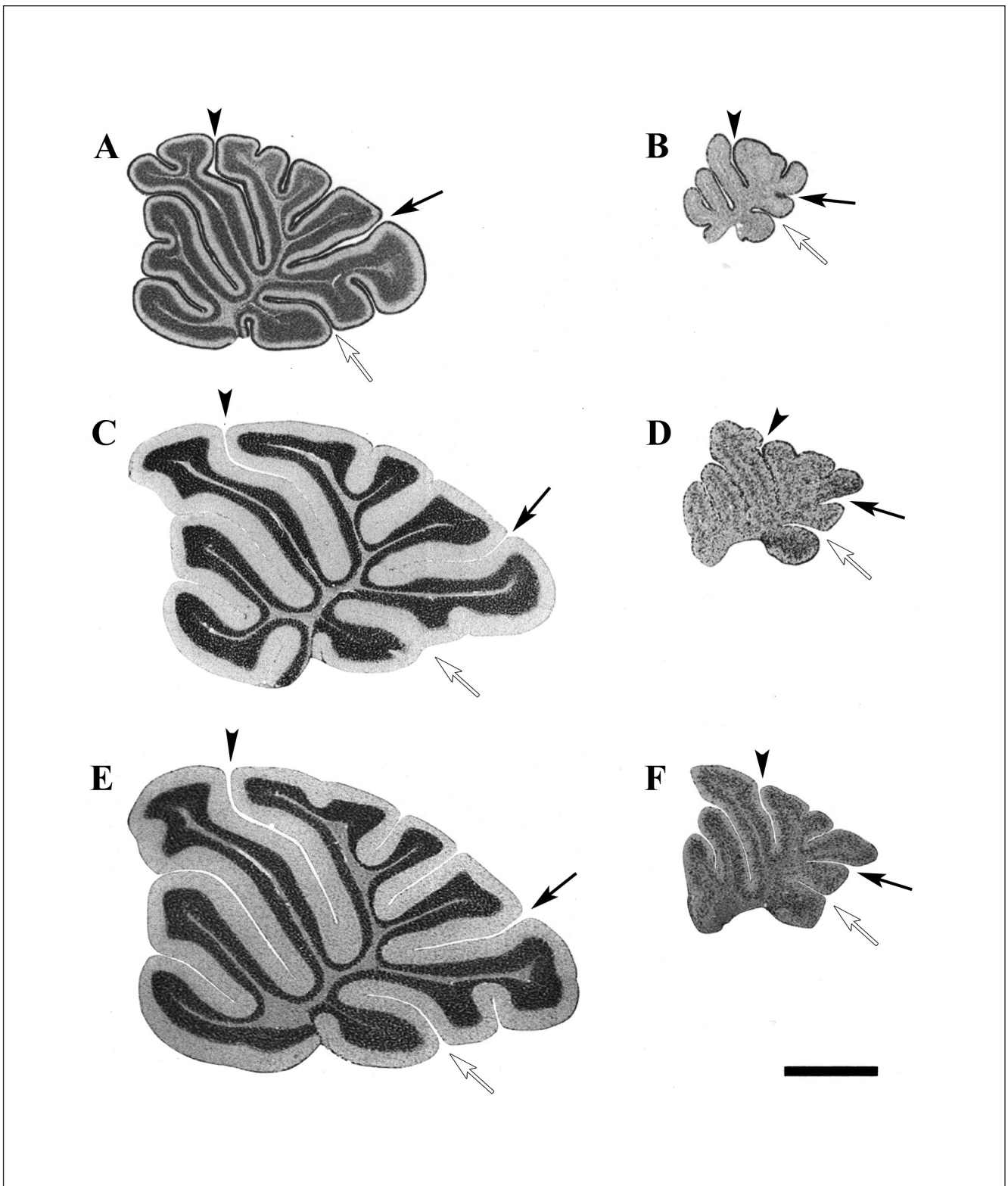

Fig 2. Photomicrographs showing the foliation patterns from +/+ (A, C, E) and *wv/wv* (B, D, F) mice. Photomicrographs A, B correspond to animals killed at P8; C and D refer to those collected at P20, and E and F to those obtained at P90. In both genotypes, the vermis is divided along the anterior-posterior axis into four lobes: the anterior ranges from the rostral pole of the cerebellar cortex to the fissure prima (arrowhead), the central lobe between the fissura prima and the fissura secunda (black arrow), the posterior lobe between the secunda and the posterolateralis (white arrow), and the inferior lobe. Scale bar – 1mm.

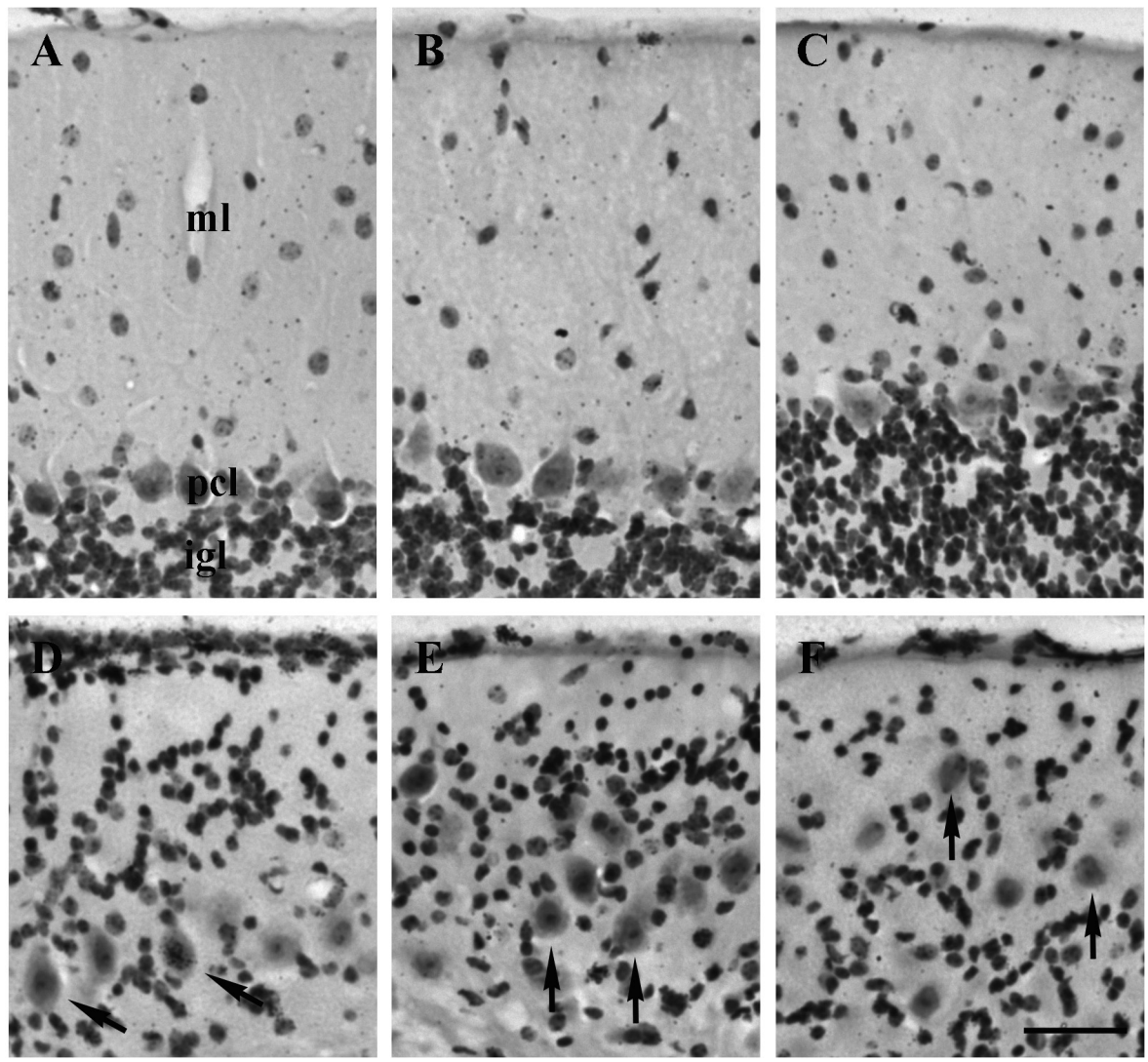

Fig 3. High-magnification photomicrographs from +/+ (A–C) and *wv/wv* (D–F) mice collected at postnatal day 90. A and D correspond to the lobule I, B and E to the lobule V, and C and F to the lobule X. D shows ectopic cells located in subpial position as well as in the middle-to-lower part of the ML. E indicates ectopic cells only settled in the middle-to-lower part of the ML and F those located randomly placed throughout the ML. ml, molecular layer; pcl, Purkinje cell layer; igl, internal granular layer. Arrows indicate Purkinje cells. Scale bar – 50 μm.

In a subsequent analysis, the PCs neurogenetic profiles were built. These arise from the decrease in the fraction of labeled PCs that took place between the above-mentioned successive ^{3}[H]TdR injection series. In Fig. 4, the frequencies of newly produced PCs are also plotted against time. Three observations can be drawn:

1) as expected, no statistical differences were observed between +/+ and *wv/wv* in any cerebellar cortex lobe over time,

2) the span of PCs neurogenesis was similar for every vermal lobe (from E10 to E14), and

3) the peak of newborn PCs was always reached toward E12.

An important consideration in the development of the lobes is to ascertain whether the final location of *wv/wv* PCs represents a random event or, on the contrary, it is related to their relative time of origin. Examination of the above-deduced developmental timetables enabled us to differentiate among neurons produced at E10 and E11, those generated at E12 and those formed at E13 and E14; corresponding to early, middle and late-born PCs, respectively. The percentages of these populations in each lobe are compared in Table IV. Two trends become

Table III. Spatial disposition of ectopic GCs in the molecular layer

	Position of ectopic cells		
Area	Subpial position	middle-to-lower part of the molecular layer	randomly placed throughout the molecular layer
Lobule I	+	–	–
Lobule III	–	+	–
Lobule V	–	+	–
Lobule VII	–	–	+
Lobule VIII	+	–	–
Lobule IX	+	–	–
Lobule X	–	–	+
F. Prima	–	+	–
F. Secunda	–	–	+
F. Posterolateralis	+	–	–

The qualitative analyzes of the cerebellar cortex were done in 14 *ww/wv* mice from different dams (7 from the E14–15 and 7 from the E15–16 [^{3}H]TdR time-windows). The symbol "+" denotes the occurrence of a pattern in a given area of the cerebellar cortex.

Table IV. Percentage of generated Purkinje cells

	Generation of Purkinje cells		
Lobe	Early-generated (E10-E11)	Middle-generated (E12)	Late-generated (E13-E14)
Anterior	8.5±1.1^a	51.4±4.0^a	40.1±1.4^a
Central	21.6±1.8^b	54.1±3.0^a	24.3±1.3^b
Posterior	19.8±2.1^b	53.9±3.5^a	26.3±1.6^b
Inferior	8.5±1.7^a	51.4±3.7^a	40.1±2.3^a

Mean ±SEM are indicated. The percentage of early, middle and late-produced Purkinje cells scored in each lobe of the cerebellar cortex. Purkinje cells formed from E10 to E11 are considered early-born, those produced at E12 are medium-generated whereas those generated from E13 to E14 are late-born. Groups tagged with different letters indicate statistically significant differences among anterior, central, posterior and inferior lobes (one-way ANOVA followed by Student-Newman-Keuls). Values are shown in Fig. 4.

apparent: 1) the proportion of middle-produced PCs did not vary and 2) the anterior and inferior lobes of the *weaver* homozygotes had more late-generated Purkinje cells than the central and posterior lobes, which, in turn, presented more early-produced ones.

DISCUSSION

To obtain information about the development of the *wv/wv* cerebellar cortex lobes, three major experimental procedures were undertaken:
1) quantitative determination of several cerebellar cortex features,
2) qualitative evaluation of the developmental changes occurring in this cortical region, and
3) an autoradiographic analysis of PCs generation and placement. The results indicate the following:
a) an important reduction in the size of the *wv/wv* cerebellum, which is in line with previous reports (Rakic and Sidman 1973a, 1973b, Martí et al. 2013). However, as distinguished from these authors, current work indicates that a significant miniaturization in all of the *wv/wv* cerebellar cortex exists,
b) the cerebellar cortex of the *weaver* homozygotes presents cytoarchitectonic anomalies depending on the age and the analyzed lobe,
c) the depletion of *wv/wv* PCs is not linked to their times of birth. This occurred in each of the analyzed cerebellar cortex lobes, and
d) the expression of the *weaver* gene does not interfere with the settled patterns of the PCs.

We propose that the miniaturization of the cerebellar cortex lobes in the *weaver* condition may be related to the loss of GCs precursors. Depletion of these neuroblasts has been reported in the *wv/wv* mice (Rezai and Yoon 1972, Rakic and Sidman 1973a, 1973b). On this matter, it has been documented in normal rats that the selective elimination of GCs precursors with X-irradiation (Altman and Bayer 1997), anti-tumor agents (Bottone et al. 2012), impairment of the thyroid status (Ahmed et al. 2010) and virus infection (Oster-Granite and Herndon 1976) produce an important reduction in the cerebellar cortex size.

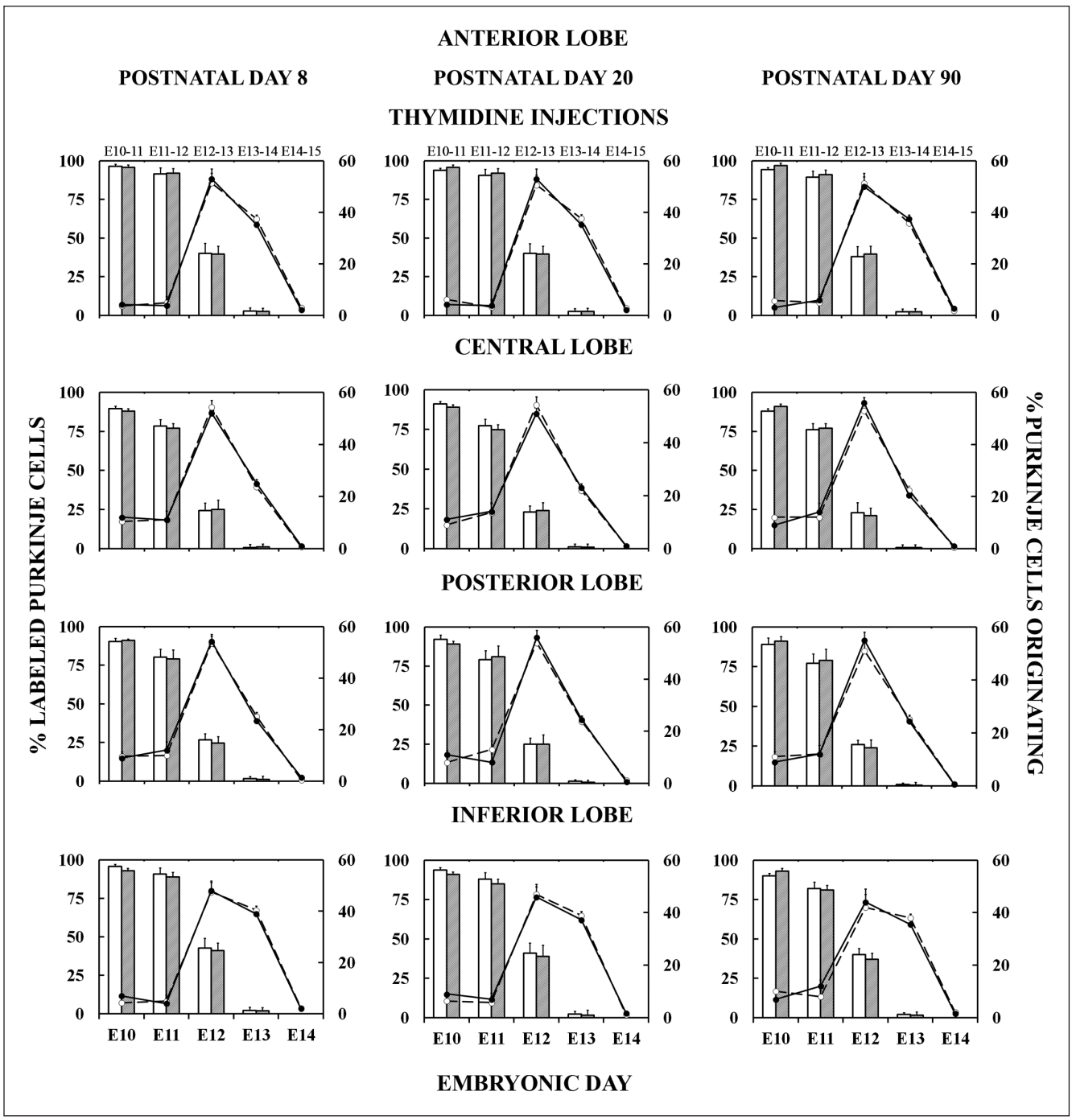

Fig 4. Comparison of cerebellar neurogenetic patterns between wild-type and *weaver* for Purkinje cells in each lobe of the cerebellar cortex at postnatal day 8, 20 and 90. Percentages are expressed as mean ±SEM. Frequency histograms of Purkinje cells labeled with tritiated thymidine on successive time-windows of the embryonic period. White and gray columns represent +/+ and *wv/wv*, respectively. The timetables of neurogenesis for +/+ (open circles and dashed lines) and *wv/wv* (closed circles and solid lines) Purkinje cells are also plotted. E: embryonic day.

Observations made at P20 revealed that the EGL was depleted of cells in the +/+ mice. However, this was not the case in any of the studied *wv/wv* cerebellar cortex lobes. Causes for the persistence of this germinal matrix are unknown. A possibility is that the loss of *wv/wv* GCs leads to continuous proliferative signals from their targets, the PCs; which may extend the period of GCs production and, in consequence, the persistence of the EGL. There is evidence indicating a powerful influence of PCs on the generative behavior of GCs precursors through secretion of sonic hedgehog (Vaillant and Monard 2009).

When the *weaver* homozygotes were collected at P90, many GCs were ectopically located in the ML. The reason why these microneurons were arrested is unknown, but the close correspondence between the altered migration of these microneurons (Rakic and Sidman 1973a, Hatten et al. 1986) and the abnormal development of their axons (Willinger and Margolis 1985, Smeyne et al. 1991) should be taken into account. We also know, from previous X-irradiation studies, that a prerequisite for the formation of ectopic GCs in the ML is the regeneration of the EGL (Altman 1973). The patterns of ectopic cell distribution reported here (Fig. 3 and Table III) may be compatible with the regeneration of this germinal matrix.

The autoradiographic results of this study confirm previous results from our laboratory (Martí et al. 2002). PCs in the weaver condition are produced from E10 to E15, suggesting that the expression of the mutant gene does not disturb the generation of these cells. This makes sense since the expression of the gene is reported to occur from E15, when PCs are already originated. The period of neurogenesis determined in this work is close to that previously reported using replication-defective adenoviral vectors (Hashimoto and Mikoshiba 2003). Moreover, in an earlier study Namba et al. (Namba et al. 2011) showed that, in normal mice, PC birth dates play an important role in organizing the cerebellum into longitudinal compartments along the mediolateral axis. Further experiments should be done to determine whether +/+ and *wv/wv* time of PCs origin profiles, inferred with [^{3}H]TdR autoradiography, determine the lateral-to-medial compartmentalization of this organ.

Our data also indicate a severe loss of PCs in the *wv/wv* cerebellum, which is in line with previous reports (Herrup and Trenkner 1987, Eisenman et al. 1998, Martí et al. 2002, 2013). However, as distinguished from these authors, it was found that:

1) the depletion of these macroneurons is not progressive with age (from P8 to P90) in any of the studied cerebellar cortex lobes, and

2) the numerical decrease of *wv/wv* PCs is regionally variable.

The most important deficit was seen in the central and posterior lobes; depletion was less observable in the anterior lobe and least observable in the inferior lobe.

How the expression of the *weaver* gene affects to these macroneurons depending on the studied lobe is not yet solved. Because its expression is reported from E15 (Wei et al. 1997), we hypothesize that the deficit of PCs might be linked to the loss of young Purkinje cells, rather than to the vulnerability of their neuroblasts. On the other hand, the expression of different isoforms (Wei et al. 1998) could account for the differential vulnerability of the lobes.

Experiments using [^{3}H]TdR autoradiography were designed to test whether the loss of *weaver* PCs in each lobe of the cerebellar cortex is related to timetables of neurogenesis of these macroneurons. Whether neurodegeneration is linked to neurogenetic timetables (systematic across age), neurogenetic patterns in the *weaver* homozygotes should be different from the wild-type group. Whether depletion is not related to timetables of neurogenesis (random across age), there should be no significant differences between the neurogenesis of Purkinje cells in the wild-type and *weaver* groups. Our data support the second possibility, suggesting that the *weaver* gene is targeting PCs irrespectively of their time of birth. This concurs with the observation that the loss of PCs in the *weaver* homozygotes is observed from E19 (Bayer et al. 1996).

Our results about the placement of *weaver* PCs confirm previous results from our laboratory (Martí et al. 2002). The novelty of this work lies in the fact that these macroneurons were distributed according to neurogenetic gradients, which were not modified from P8 to P90. We have also observed that a tendency to the accumulation of late-produced PCs in the anterior and posterior lobes exists, whereas early-generated ones were concentrated in the central and inferior lobes. These results suggest that the *wv/wv* PCs may migrate properly to their final destinations.

The *weaver* homozygotes have been studied as an animal model of hereditary ataxias (Grüsser-Cornehls and Bäule 2001, Manto and Marmolino 2009, Cedelin 2014). Because the different molecular mechanism behind each type of ataxia, extrapolation of the results using the *weaver* animal model is not straightforward. However, as patients affected with this condition present an important demise of PCs their depletion could be regionally variable along the vermis and not related to neurogenesis timetables.

CONCLUSIONS

All of the cerebellar cortex lobes are affected by the expression of the *weaver* gene with several age-dependent alterations in the cytoarchitectonics. Incomplete migration of GCs occurred and this led to the generation of ectopic GCs in the *wv/wv* ML. On the other hand, the birth sequences of postmitotic PCs, as well as their spatial distribution, were similar for +/+ and *wv/wv* in every studied age and cerebellar lobe. Thus, the expression of the *weaver* gene affects neither the neurogenetic gradients nor migration of these macroneurons, although their depletion is regionally variable along the vermis.

As a general conclusion, age-dependent alterations in the cytoarchitecture of *wv/wv* cerebellar cortex occur while maintaining PCs developmental timetable.

ACKNOWLEDGMENT

The authors are very grateful to Dr. Bernardino Ghetti for providing the mice. This research was supported by grants, FIS-PI-13-01330, and SGR2014-00885.

REFERENCES

Ahmed OM, Abd El-Tawab SM, Ahmed RG (2010) Effects of experimentally induced maternal hypothyroidism and hyperthyroidism on the development of rat offspring: I. The development of the thyroid hormones-neurotransmitters and adenosinergic system interactions. Int J Dev Neurosci 28: 437–454.

Altman J (1973) Experimental reorganization of the cerebellar cortex III. Regeneration of the external germinal layer and granule cell ectopia. J Comp Neurol 149: 153–180.

Altman J, Bayer SA (1997) Development of the Cerebellar System: In Relation to its Evolution, Structure and Functions. CRC Press, Inc. Boca Raton, USA.

Armstrong C, Hawkes R (2001) Selective Purkinje cell ectopia in the cerebellum of the weaver mouse. J Comp Neurol 439: 151–161.

Bayer SA, Altman J (1987) Directions in neurogenetic gradients and patterns of anatomical connections in the telencephalon. Prog Neurobiol 29: 57–106.

Bayer SA, Wills KV, Wei J, Feng Y, Dlouhy SR, Hodes ME, Verina T, Ghetti B (1996) Phenotypic effects of the weaver gene are evident in the embryonic cerebellum but not in the ventral midbrain. Brain Res Dev Brain Res 96: 130–137.

Blatt BJ, Eisenman LM (1985) A quantitative and quantitative light microscopic study of the inferior olivary complex of normal, reeler, and weaver mutant mice. J Comp Neurol 232: 117–128.

Bottone MG, Veronica DB, Piccolini VM, Bottiroli G, De Pascali SA, Fanizzi FP, Bernocchi G (2012) Developmental expression of cellular prion protein and apoptotic molecules in the rat cerebellum: effects of platinum compounds. J Chem Neuroanat 46: 19–29.

Cavalcanti-Kwiatkoski R, Raisman-Vozari R, Ginestet L, Del Bel E (2010) Altered expression of neuronal nitric oxide synthase in weaver mutant mice. Brain Res 1326: 40–50.

Cedelin J (2014) From mice to men: lessons from mutant ataxic mice. Cerebellum Ataxias 1: 4 [doi:10.1186/2053-8871-1-4].

Chedotal A (2010) Should I stay or should I go? Becoming a granule cell. Trends Neurosci 33: 163–172.

Cheng SV, Nadeau JH, Tanzi RE, Watkins PC, Jagadesh J, Taylor BA, Haines JL, Sacchi N, Gusella JF (1988) Comparative mapping of DNA markers from familial Alzheimer disease and Down syndrome regions of human chromosome 21 to mouse chromosomes 16 and 17. Proc Natl Acad Sci USA 85: 6032–6036.

Eisenman LM, Gallagher E, Hawkes R (1998) Regionalization defects in the weaver cerebellum. J Comp Neurol 394: 431–444.

Goldowitz D, Hamre K (1998) The cells and molecules that make a cerebellum. Trends Neurosci 21: 375–382.

Grüsser-Cornehls U, Bäule J (2001) Mutant mice as a model for cerebellar ataxia. Progress in Neurobiology 63: 489–540.

Harkins AB, Fox AP (2002) Cell death in weaver mouse cerebellum. Cerebellum 3: 201–206.

Harrison SM, Roffler-Tarlov S K (1998). Cell death during development of testis and cerebellum in the mutant mouse weaver. Dev Biol 195: 174–178.

Hashimoto M, Mikoshiba K (2003) Mediolateral compartmentalization of the cerebellum is determined on the birth date of Purkinje cells. J Neurosci 23: 11342–11351.

Hatten ME, Liem RKH, Mason CA (1986) Weaver mouse cerebellar granule neurons fail to migrate on wild-type astroglial processes in vitro. J Neurosci 6: 2676–2683.

Herrup K, Trenkner E (1987) Regional differences in cytoarchitecture of the weaver cerebellum suggest a new model for weaver gene action. Neuroscience 23: 871–885.

Lalonde R, Strazielle C (2007) Spontaneous and induced mouse mutations with cerebellar dysfunctions: behavior and neurochemistry. Brain Res 1140: 51–74.

Lange W (1982) Regional differences in the cytoarchitecture of the cerebellar cortex. In: The cerebellum: new vistas (Palay SL CV, Ed.). Springer-Verlag, Berlin, Germany. p. 93–107.

Larsell O (1952) The morphogenesis and adult pattern of the lobules and fissures of the cerebellum of the white rat. J Comp Neurol 97: 281–356.

Leto K, Rolando C, Rossi F (2012) The genesis of cerebellar GABAergic neurons: fate potential and specification mechanisms. Front Neuroanat 6: 6 [doi: 10.3389/fnana.2012.00006].

Manto M, Marmolino D (2009) Animal models of human cerebellar ataxias: a cornerstone for the therapies of the twenty-first century. Cerebellum 8: 137–154.

Maricich SM, Soha J, Trenkner E, Herrup K (1997) Failed cell migration and death of Purkinje cells and deep nuclear neurons in the weaver cerebellum. J Neurosci 17: 3675–3683.

Martí J, Santa-Cruz MC, Bayer SA, Ghetti B, Hervas JP (2007) Purkinje cell age-distribution in fissures and in foliar crowns: a comparative study in the weaver cerebellum. Brain Struct Funct 212: 347–357.

Martí J, Santa-Cruz MC, Molina V, Serra R, Bayer SA, Ghetti, B and Hervás JP (2009) Regional differences in the vulnerability of substantia nigra dopaminergic neurons in weaver mice. Acta Neurobiol Exp (Wars) 69: 198–206.

Martí J, Santa-Cruz MC, Serra R, Valero O, Molina V, Hervás JP, Villegas S (2013) Principal component and cluster analysis of morphological variables reveals multiple discrete sub-phenotypes in weaver mouse mutants. Cerebellum 12: 406–417.

Martí J, Wills KW, Ghetti B, Bayer SA (2001) Evidence that the loss of Purkinje cells and deep cerebellar nuclei neurons in homozygous weaver is not related to neurogenetic patterns. Int J Dev Neuroscience 19: 599–610.

Martí J, Wills KV, Ghetti B, Bayer SA (2002) A combined immunohistochemical and autoradiographic method to detect midbrain dopaminergic neurons and determine their time of origin. Brain Res Brain Res Protoc 9: 197–205.

Namba K, Sugihara I, Hashimoto M (2011) Close correlation between the birth date of Purkinje cells and the longitudinal compartmentalization of the mouse adult cerebellum. J Comp Neurol 519: 2594–2614.

Oster-Granite ML, Herndon RM (1976) The pathogenesis of parvovirus-induced cerebellar hypoplasia in the Syrian hamster, Mesocricetus auratus. Fluorescent antibody, foliation, cytoarchitecture, Golgi and electron microscopic studies. J Comp Neurol 169: 481–521.

Ozaki M, Hashikawa T, Ikeda K, Miyakawa Y, Ichikawa T, Ishihara Y, Kumanishi T, Yano R (2002) Degeneration of pontine mossy fibers during cerebellar development in weaver mutant mice. Eur J Neurosci 16: 565–574.

Patil N, Cox DR, Bhat D, Faham M, Myers RM, Peterson AS (1995) A potassium channel mutation in weaver mice implicates membrane excitability in granule cell differentiation. Nat Genet 11: 126–129.

Rakic P, Sidman RL (1973a) Sequence of development abnormalities leading to granule cell deficit in cerebellar cortex of weaver mutant mice. J Comp Neurol 152: 103–132.

Rakic P, Sidman RL (1973b) Organization of cerebellar cortex secondary to deficit of granule cells in weaver mutant mice. J Comp Neurol 152: 133–162.

Reeber SL, Otis, TS, Sillitoe RV (2013) New roles for the cerebellum in heath and disease. Front Syst Neurosci 7: 83 [doi: 10.3389/fnsys.2013.00083].

Reeves RH, Crowley MR, Lorenzon N, Pavan WJ, Smeyne RJ, Goldowitz D (1989) The mouse neurological mutant weaver maps within the region of chromosome 16 that is homologous to human chromosome 21. Genomics 5: 522–526.

Rezai Z, Yoon CH (1972) Abnormal rate of granule cell migration in the cerebellum of weaver mutant mice. Dev Biol 29: 17–26.

Schein JC, Hunter DD, Roffler-Tarlov S (1998) Girk2 expression in the ventral midbrain, cerebellum, and olfactory bulb and its relationship to the murine mutation weaver. Dev Biol 204: 432–450.

Schilling K, Oberdick J, Rossi F, Baader SL (2008) Besides Purkinje cells and granule neurons: an appraisal of the cell biology of the interneurons of the cerebellar cortex. Histochem Cell Biol 130: 601–615.

Sekigucchi M, Nowakowski RS, Nagato Y, Tanaka O, Guo H, Madoka M, Abe H (1995) Morphologial abnormalities in the hippocampus of the weaver mutant mouse. Brain Res 696: 262–267.

Smeyne RJ, Pickford LB, Rouse RV, Napieralski J, Goldowitz D (1991) Abormalities in premigratory granule cells in the weaver cerebellum defined by monoclonal OZ42. Anat Embryol (Berl) 183: 213–219.

Triarhou LC, Norton J, Ghetti B (1988) Mesencephalic dopamine cell deficit involves areas A8, A9 and A10 in weaver mutant mice. Exp Brain Res 70: 256–265.

Vaillant C, Monard D (2009) SHH pathway and cerebellar development. Cerebellum 8: 291–301.

Verina T, Tang X, Fitzpatrick L, Norton J, Vogelweid CM, Ghetti B (1995). Degeneration of Sertoli and spermatogenic cells in homozygous and heterozygous weaver mice. J. Neurogenet 9: 251–265.

Wahlsten D, Andison M (1991) Patterns of cerebellar foliation in recombinant inbred mice. Brain Res 557: 184–189.

Wei J, Dlouhy S R, Bayer S, Piva R, Verina T, Wang Y, Feng Y, Dupree B, Hodes ME, Ghetti B (1997) In situ hybridization analysis of Girk2 expression in the developing central nervous system in normal and weaver Mice. J Neuropathol Exp Neurol 56: 762–771.

Wei J, Hodes ME, Piva R, Feng Y, Wang B, Ghetti B (1998) Characterization of murine Girk2 transcript isoforms: structure and differential expression. Genomics 51: 379–390.

Wei J, Hodes ME, Wang Y, Feng Y, Ghetti B, Dlouhy SR (1996) cDNA selection with DNA microdissected from mouse chromosome 16: isolation of novel clones and construction of a partial transcription map of the C3-C4 region. Genome Res 6: 678–687.

Whorton MR, Mackkinnon R (2013). X-ray structure of the mammalian GIRK2-βγ G-protein complex. Nature 498: 190–197.

Willinger M, Margolis DM (1985). Effect of the weaver (wv) mutation on cerebellar neuron differentiation. II. Quantification of neuron behavior in culture. Dev Biol 107: 173–179.

Wullimann MF, Mueller T, Distel M, Babaryka A, Grothe B, Köster RW (2011) The long adventurous journey of rhombic lip cells in jawed vertebrates: a comparative developmental analysis. Front Neuroanat 21: 5–27.